III International Conference on Particle-based Methods – Fundamentals and Applications
PARTICLES 2013
M. Bischoff, E. Oñate, D.R.J. Owen, E. Ramm & P. Wriggers (Eds)

DIE FILLING PROCESS SIMULATION USING DISCRETE ELEMENT METHOD (DEM)

NASATO D. S.[*], GONIVA C.[1,2], KÖNIG B.[1], PIRKER S.[1,3], KLOSS C.[1,2]

[*] Christian-Doppler Laboratory on Particulate Flow Modelling
Institute of Fluid Mechanics and Heat Transfer, Johannes Kepler University - JKU
Altenbergerstrasse 69, 4040 Linz, Austria
e-mail: daniel.schiochet_nasato@jku.at, web page: http://www.particulate-flow.at

[1]Christian-Doppler Laboratory on Particulate Flow Modelling
Institute of Fluid Mechanics and Heat Transfer
Johannes Kepler University – JKU
Altenbergerstrasse 69, 4040 Linz, Austria
e-mail: stefan.pirker@jku.at , web page: http://www.particulate-flow.at

[2]DCS Computing GmbH
Altenbergerstr. 66a – Sciencepark, 4040 Linz, Austria
e-mail:office@dcs-computing.com, web page: www.dcs-computing.com

[3]Institute of Fluid Mechanics and Heat Transfer
Johannes Kepler University - JKU
Altenbergerstrasse 69, 4040 Linz, Austria
e-mail: office.fluid@jku.at, web page: http://fluid.jku.at

Key words: DEM, Wet Sand, Die Filling, Coarse Grain.

1 INTRODUCTION

Powder compaction and sintering are important techniques for the mass production of geometrically complex parts. Powder is poured from a reservoir into the feeding shoe, which then passes the cavity one or more times thereby delivering powder into it. The powder is then compressed to create a relatively brittle green body. Finally, the green body is ejected from the cavity and sintered in a furnace where thermal activation below the melting point produces a fully dense structure. Necks form and grow between adjacent grains thereby eliminating the porosity of the part. In general, a consistent and uniform die filling process is always desirable. Heterogeneity during die filling can propagate through the subsequent processes and finally lead to serious product defects, such as cracking, low strength, distortion and shrinkage [1].

Capillary cohesion is known to influence strongly the strength and flow properties of granular materials. At low levels of water content, the water forms a discontinuous phase composed of interparticle bridges that are unevenly distributed in the bulk (the pendular state) [2].

For powder filling process these capillary forces may have strong influence in the particle dynamics and subsequent packing. An approach using discrete element method (DEM) simulation is proposed to reproduce die filling process and investigate process characteristics

that affect final sand cake shape and may lead to in-homogeneities in powder during the filling process. Also an experimental apparatus able to reproduce the die filling process was built to validate numerical model. A coarse grain model is also necessary to reduce the model size (reduce the number of particles).

2 CAPILLARY FORCES

In the frame of the CFDEM-project (www.cfdem.com) [3], the open source DEM code LIGGGHTS is being developed [4]. It is based on the molecular dynamics (MD) code LAMMPS [5], a parallel particle simulator at the atomistic, meso, or continuum scale. A capillary force model was implemented in the LIGGGHTS DEM code version 2.3. This capillary model is based on the work of Richefeu et al. [2]. The capillary attraction force between two particles is a consequence of the liquid surface tension and the pressure difference between liquid and gas phases. For efficient numerical calculation, we need an explicit expression of the capillary force f_n^c as a function of the interparticle gap δ_n. The capillary force can be cast in the following form [2]:

$$f_n^c = \begin{cases} -\pi\gamma_S\sqrt{R_1R_2}[\exp(A\delta_n^* + B) + C] & for\ \ \delta_n^* > 0, \\ -\pi\gamma_S\sqrt{R_1R_2}[\exp(B) + C] & for\ \ \delta_n^* \leq 0 \end{cases} \quad (1)$$

where R_1 and R_2 are the sphere radii ($R_1 \leq R_2$), γ_s is the liquid surface tension and $\delta_n^* = \delta_n/R_2$. The parameters A, B, and C are functions of the liquid volume V_b of the bond and the contact angle θ as follows [2]:

$$A = -1.1(V_b^*)^{-0.53} \quad (2)$$

$$B = (-0.148\, ln\, V_b^* - 0.96)\theta^2 - 0.0082\, ln\, V_b^* + 0.48 \quad (3)$$

$$C = 0.0018\, ln\, V_b^* + 0.078 \quad (4)$$

where $V_b^* = V_b/R_2^3$.

It can be shown that a liquid bond is stable as long as the gap is below a debonding distance δ_n^{max} given by [2]:

$$\delta_n^{max} = (1 + 0.5\theta)V_b^{1/3} \quad (5)$$

3 COARSE GRAIN MODEL

In order to reduce this number of particles and consequently the simulation time, a coarse grain model was proposed to reduce the number of particles keeping the quality of the results. The coarse grain model is described briefly as follows [6]. As shown in Figure 1, l^3 original particles are emulated by a coarse grain particle in the CGM with coarse grain ratio l. The coarse grain particle and its original particles are supposed to move for the same direction in translation in the CGM (Figure 1a). Each original particle is supposed to rotate around its center. These particles are supposed not to rotate around the center of the coarse grain particle (Figure 1b) [6].

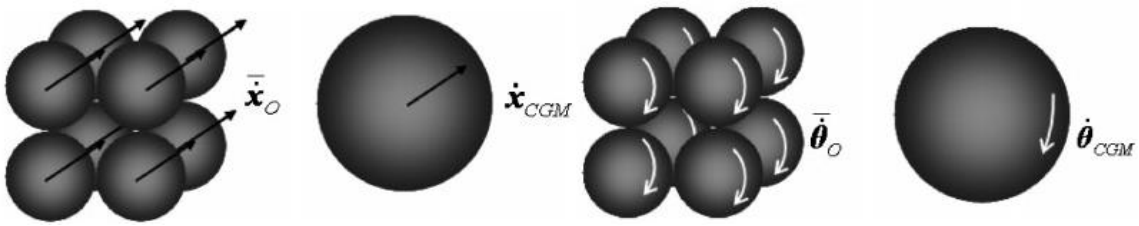

(a) Translation (b) Rotation

Figure 1: Coarse grain model (l=2) [6].

The translational and rotational movements of particles are modeled as [6]:

$$\frac{1}{2}m_{CGM}\dot{x}_{CGM}^2 + \frac{1}{2}I_{CGM}\dot{\theta}_{CGM}^2 = l^3\left(\frac{1}{2}m_{Org}\dot{x}_{Org}^2 + \frac{1}{2}I_{Org}\dot{\theta}_{Org}^2\right) \quad (6)$$

where m, $\boldsymbol{x}$, I and $\boldsymbol{\theta}$ are mass, position vector, moment of inertia and rotational angle of a particle. The subscript *CGM* and *Org* are for coarse grain particle and original particle. Equation (6) means that the kinematic energy of the coarse grain particle and the kinematic energy of the original particles are equal, and the force on a coarse grain particle is l^3 times stronger than those of original particles. The forces on the coarse grain particles are [6]:

$$m_{CGM}\ddot{x}_{CGM} = l^3 m_{Org}\ddot{x}_{Org} \quad (7)$$

$$m_{CGM}\ddot{x}_{CGM} = l^3\sum F_{cOrg} + l^3 F_{gOrg} \quad (8)$$

where F_c and F_g are force between particle-particle and force of gravity. Equation (8) means a collision between two coarse grain particles is equivalent to collisions of each original particle.

The same way it was proposed to have the capillary forces to scale in the same ratio (l^3) as the contact force. The capillary force was plotted for different radius size and it was verified that its relations with the scale factor is 0.95 l + 0.056. Our proposal for coarse grain is to keep the same scale relation as for the contact force l^3. This way a coarse grain factor (CGF) was applied to the capillary force which corrects the calculated capillary force to keep the same force relation. This CGF was obtained by the ratio of the contact and the capillary force for different scale up factors. Equation (9) means the coarse grain capillary force and its relation with the original capillary force.

$$f_{nCGM}^{C} = f_{nOrig}^{C} l^{2.0142} \quad (9)$$

where f_{nCGM}^{C} means the capillary force of the coarse grain and f_{nOrig}^{C} means the capillary force of the original system.

4 MODEL CALIBRATION

Generally, experimentally measured parameter values provide a good starting point for calibrating the DEM model parameters. Applying those parameters although can produce disappointing results via the DEM model. To ensure the validity of results obtained from DEM simulations, a three-step approach should be used: i) the DEM parameters are obtained from calibration experiments, ii) a validation experiment that exhibits similar physics compared to the real scale is used to check the DEM parameters, and iii) the set of parameters

is used for the simulation of the production process.

Since experimental measurements are typically of bulk-type character and DEM is requiring parameters for the individual contacts in the particulate system the DEM concept represents an approximation of a real-life bulk system. Additionally, some factors may not be considered in the contact model of the DEM approach such as permanent deformation, crushing, and surface roughness, but its effects have to be considered in the model. Because of the wide variety of different DEM models used – all with their own set of parameters – there is no publically available database for suitable interaction parameters. Subsequently, the method adopted for calibration is the following: i) experimentally measure or visually record a required behavior, ii) create a test with DEM that will introduce similar behavior, iii) put in a set of input parameter values and run a simulation, iv) assess the results obtained this way, v) return to step i, modify one or more parameters and vi) repeat steps iii to v until correct parameters values have been obtained. Experiments are recommended to be in small scale, thus, allowing for reduced simulation times and handling of greater sets of DEM parameters that can be tested [7].

4.1 Calibration Process

For this work metallic powder used in the die filling process was substituted by sand. The material used in the present work is sand F32 standard from Quarzwerke®. Particle size distribution is depicted in Table 1.

Table 1: Standard F32 sand size distribution.

Diameter (mm)	%
> 0.355	5
0.25-0.355	28
0.18-0.25	49
0.125-0.18	16
0.09-0.125	2

During the calibration process dry sand was used and a coarse grain factor of 5 (the same size distribution showed in Table 1 was adopted, but using particle diameter 5 times bigger). This is the same scale factor adopted for further numerical validation. For the calibration process inclined plate test and repose angle test were used. The inclined plate test consist of putting some particulate material onto a flat surface and incline this surface up to the point when the particles start sliding or rolling (threshold inclination angle). The same procedure is done by numerical simulations and the coefficients of rolling and static friction, respectively, for particle to plate surface are tuned until the same threshold inclination angle is reached

For the inclined plate tests, about 8 g of sand is put onto a flat steel surface. The surface is then inclined and particles start sliding at an angle of 22°. At 27° about 35% of the material had already slid. At about 37° there was no more material onto the surface. For the simulation runs 29° (about 50% of the material had slid) was considered as the sliding angle. The simulation with calibrated results can be seen in Figure 2.

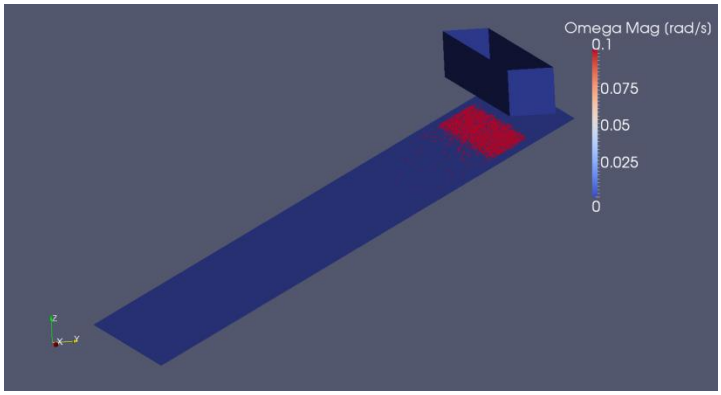

Figure 2: Angular movement [rad/s] is predicted for all particles via DEM simulation to indicate rolling movement.

The second calibration experiment is made for measuring the repose angle of the particulate material. With the coefficients of rolling and static friction, respectively, between particle and wall surface obtained from the inclined plate experiment, the coefficients of static friction and the rolling friction, respectively, for particle to particle interaction are tuned with the help of simulations of the repose angle experiment. For the repose angle measurement 72 g of sand is put into a steel cylinder of 43 mm in diameter. The steel cylinder is then removed and the repose angle is measured to be about 28°, see Figure 3a. Some simulations are done using different sets of coefficients of static and rolling friction, respectively, for calibration of the particle to particle contact. The final simulation result can be seen in Figure 3b. The final set of calibrated DEM parameters for the sand can be seen in Table 2. Other parameters also adopted in the DEM simulations can be found in Table 3.

(a)  (b) 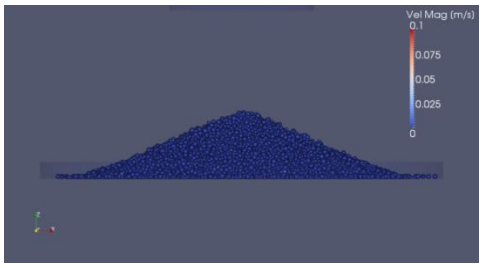

Figure 3: Final configuration of the sand bed in a repose angle experiment adopting 72 g of sand: (a) Measured repose angle in the experiment and (b) repose angle as predicted via DEM simulation.

Table 2: Calibrated parameters adopted for DEM simulations.

	particle-particle	particle-surface
Coeff. static friction [-]	0.70	0.61
Coeff. rolling friction [-]	0.50	0.50
Coeff. Restitution [-]	0.10	0.15

Table 3: Other material parameters used in the DEM simulations.

	particle material	surface material
Density [kg/m^3]	2650	7800
Poisson ratio [-]	0.3	0.3
Young's modulus [Pa]	5.00E+06	7.00E+10

4.2 Validation experiment

For validating the DEM model parameter calibration that come from calibration experiments such as i) to v) as given above a validation experiment is needed for evaluation of the quality of DEM model calibration under conditions being representative for the real-life filling process intended to be simulated. In the following a new validation experiment is described on the basis of a die filling process capturing the core physical phenomena of the corresponding industrial process. This simplified substitute system is designed to handle particulate materials of non-cohesive and cohesive characteristics as well and allows to experimentally measures and, subsequently, numerically reproduces the particle bed geometry, i.e. the spatial distribution of the repose angle, in the as-filled condition thus acting as a basis for validation of the corresponding numerical model of the filling process. In principle, the experimental setup contains two sections – a particle conditioning section and a die filling section, see Figure 4. In the particle conditioning section a defined mass of dry material is filled into a cylindrical shoe. During conditioning this packed bed is aerated by wetted air until the off-gas analysis signalizes a steady state situation, see Figure 4a. After conditioning the weight of the shoe and the wetted particulate material is measured in order to characterize the actual water content inside the material bed. In a next step, the shoe containing the now well-conditioned material is moved over the cylindrical die by a pneumatic cylinder. It is worth noting that only one passage is realized in order to produce significant inhomogeneities in the material bed, see Figure 4b. Optionally, a stamp with a well-defined weight is lowered onto the material in the die for a defined time-slot and then raised again to be able producing different states of pre-compaction, see Figure 4c and Figure 4d. After this the opening above the die is closed in order to guarantee a well-defined lightening of the subsequent optical measurements and the cylindrical side wall is slowly lowered, see Figure 4e.

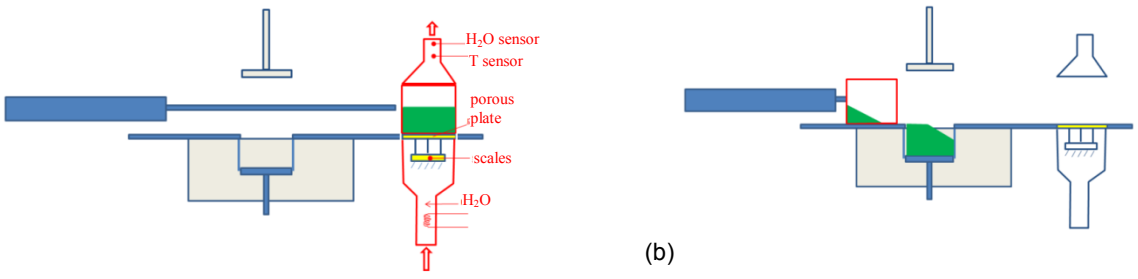

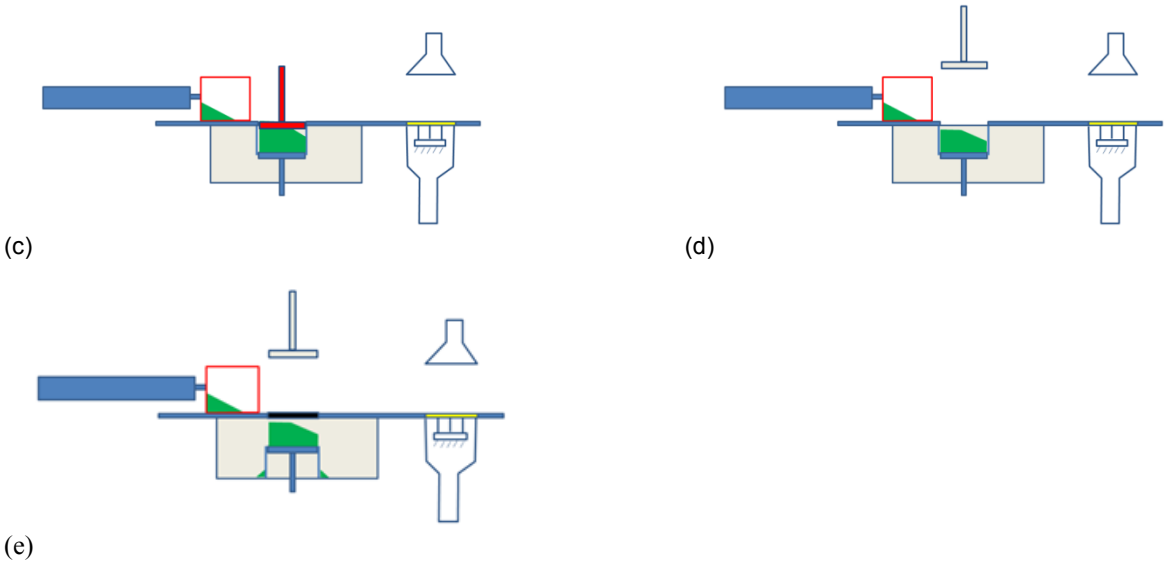

Figure 4: Sketch of an experimental setup for a validation experiment representing a simplified substitution system for an industrial die filling process: Sequence of (a) material conditioning, (b) die filling, (c) – (d) pre-compaction, (e) die opening.

5 NUMERICAL VALIDATION

The volume V_b attributed to a capillary bond between two particles is taken to be proportional to the particle diameters and the intercenter distance, and such that the total volume of all liquid bonds in the sample is equal to that of the added water. Since all particle pairs within the debonding distance are considered, the liquid coordination number z obtained by this procedure has the highest possible value. For our simulations we get z=8 for w=0.05. Also, the contact angle θ with a good approximation was set to zero. During filling process, the number of liquid bonds evolves and the available liquid must be redistributed in the system. We simply apply the above procedure every time the contact list is updated.

The validation of the calibrated DEM model for the sand is now done via the validation experiment as described above. No compaction is applied. A sample of 225 g of sand with 5% of water was prepared and left under agitation during 5 minutes for homogeneous distribution of the water and the liquid bridges formed. The adopted feeding shoe and the die cylinder both have 10 cm in diameter and 10 cm in height. The feeding shoe velocity being used in the measurements is 0.0405 m/s. This velocity is small enough to completely empty the feeding shoe.

The profile of the sand bed being formed in the experiment after complete opening is shown in Figure 5a. The tests with the sand show an uneven distribution of the material in the die cylinder. Most of the material is deposited in the first half of the cylinder with respect to the moving direction of the feeding shoe. This is primarily a consequence of the rather low velocity assigned to the feeding shoe.

A significant difference when comparing experimental and numerical result can be seen in the border regions. This might be explained by some difference in the measured velocity during filling process, which may lead to a higher material accumulation in the first half of the die cylinder for the simulation case Figure 5b. For comparison we evaluate angle formed

more in the central region of the bed (detail in the black line). For the measured data it was found an angle of 33.8° and for the numerical result it was found an angle of 32.9°.

When comparing the right region of both pictures, an angle near to 90° is depicted for both cases. For the simulations about 10% of the material was lost after the die cylinder opening most due to the collapse of the left region pile (higher pack height). In the experiments this material lost was not significant (about 2%).

(a) 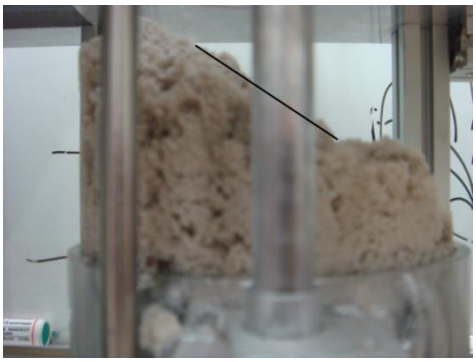 (b) 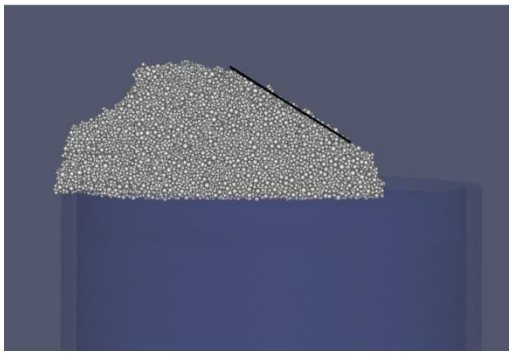

Figure 5: (a) Left side view of the profile of the sand bed as formed in the experiment (b) as predicted via the calibrated DEM model. Note that the movement of the feeding shoe is from the left to the right.

6 CONCLUSIONS

The bed angle could be reproduced with similar values for central region of the cake profile from numerical and experimental data (33.8° for the experimental data and 32.9° for the numerical result). The right border region also showed similar results with angles of approximately 90°. The left border region although showed different results when comparing to experimental data. This might be related to the fact that sand particles were simulated as spheres, and some packing resultant of the non sphericity of the real sand particles could not be captured with current numerical model. Some more measurements of the feeding show velocity may also be necessary, since for the simulations more material seem to accumulate in the first half part of the die cylinder. This velocity is a result of the pneumatic equipment that moves the feeding shoe and might varies as the feeding shoe is emptied during die feeding process. This was not considered in the model.

The proposed approach points to physically correct results. However further refinements are necessary to improve the results and other validation tests are under development.

7 REFERENCES

[1] C. Bierwisch, T. Kraft, H. Riedel, M. Moseler, “Die filling optimization using three-dimensional discrete element modelling”. Powder Technology 196, 169–179 (2009).

[2] V. Richefeu, M. S. E. Youssoufi, F. Radjai, “Shear strength properties of wet granular materials”. PHYSICAL REVIEW E 73, 051304 (2006).

[3] C. Goniva, C. Kloss, N. G. Deen, J. A.M. Kuipers, S. Pirker, Influence of rolling friction on single spout fluidized bed simulation, Particuology, 10 (5), 582-591, (2012).

[4] C. Kloss, C. Goniva, A. Hager, S. Amberger, S. Pirker, Models, algorithms and validation for opensource DEM and CFD-DEM, Progress in Computational Fluid Dynamics, 12 (2/3) 140-152, (2012)

[5] S. J. Plimpton, Fast Parallel Algorithms for Short-Range Molecular Dynamics, J. Comp. Phys., 117, 1-19, (1995)
[6] M. Sakai, Y. Yamada, Y. Shigeto, K. Shibata, V. M. Kawasaki, S. Koshizuka, "Large-scale discrete element modeling in a fluidized bed". Int. J. Numer. Meth. Fluids 2010; 64:1319–1335 (2010).
[7] C. Grohs, A. Plankensteiner, D. Schiochet Nasato, C. Kloss, "Numerical Simulation of Refractory Metals and Cemented Carbides in the Regime of Powder Filling and Powder Transfer". Plansee® Seminar 2013 – Reutte, Austria (2013).